

Electronic Supplementary Information

Molecular Origin of High-Concentration Cellulose Dissolution in Organic Acid Media: A Combined Experimental and Computational Study

Kanta Hayashi,^a Tomoya Tashiro,^a Tomohiro Hashizume,^b Takashi Watanabe,^{c,d} and Kenta Fujii^{a}*

^a Graduate School of Sciences and Technology for Innovation, Yamaguchi University, 2-16-1 Tokiwadai, Ube, Yamaguchi 755-8611, Japan. ^b Daicel Corporation, Ofuka-Cho, Kita-Ku, Osaka 530-0011, Japan. ^c Research Institute for Sustainable Humanosphere, Kyoto University, Uji, Kyoto 611-0011, Japan. ^d Biomass Product Tree Industry-Academia Collaborative Research Laboratory, Kyoto University, Uji, Kyoto 611-0011, Japan.

** To whom correspondence should be addressed. E-mail: k-fujii@yamaguchi-u.ac.jp*

Experimental and Computational Methods.

High-energy X-ray total scattering (HEXTS). HEXTS measurements were conducted at ambient temperature using a high-energy X-ray diffraction apparatus installed at SPring-8 (BL04B2 beamline, JASRI, Japan). Monochromatized 61.19 keV X-rays were obtained using a Si(220) monochromator. The observed X-ray scattering intensities were corrected for absorption, polarization, and incoherent scattering to determine coherent scattering intensities, $I_{\text{coh}}(q)$.¹⁻³ The experimental X-ray structure factor per stoichiometric volume, $S^{\text{exp}}(q)$, was obtained using the following equation:

$$S^{\text{exp}}(q) = \frac{\frac{I_{\text{coh}}(q)}{N} - \sum n_i f_i(q)^2}{\{\sum n_i f_i(q)\}^2} + 1 \quad (\text{S1}),$$

where n_i and $f_i(q)$ correspond to the number and atomic scattering factor of atom i , respectively, and N is the total number of atoms in the stoichiometric volume. The radial distribution function, $G^{\text{exp}}(r)$ is obtained using the Fourier transform of the $S^{\text{exp}}(q)$ as follows:

$$G^{\text{exp}}(r) - 1 = \frac{1}{2\pi^2 r \rho_0} \int_0^{q_{\text{max}}} q \{S^{\text{exp}}(q) - 1\} \sin(qr) W(q) dq \quad (\text{S2}),$$

where ρ_0 is the number density of atoms, q_{max} is the maximum value of q (25 \AA^{-1} in this study), and $W(q)$ corresponds to the Lorch window function.⁴

Table S1. Concentrations (weight percent and molarity), density (d) and refractive index (n_2) of CB/FA, CL/FA, CB/PA, and CL/PA solutions. c_{CB} and c_{CB}' denote the molarity of CB and the CB dimer-equivalent molarity of CL.

| CB/FA solutions | | | |
|-------------------------------|---------------------------------------|------------------------|-------|
| $w_{\text{CB}} / \text{wt}\%$ | $c_{\text{CB}} / \text{mol dm}^{-3}$ | $d / \text{g cm}^{-3}$ | n_2 |
| 0 | 0 | 1.211 | 1.368 |
| 20 | 0.614 | 1.261 | 1.397 |
| 30 | 0.872 | 1.293 | 1.406 |
| 40 | 1.090 | 1.306 | 1.417 |
| 50 | 1.284 | 1.318 | 1.422 |
| CL/FA solutions | | | |
| $w_{\text{CL}} / \text{wt}\%$ | $c_{\text{CB}}' / \text{mol dm}^{-3}$ | $d / \text{g cm}^{-3}$ | n_2 |
| 5 | 0.179 | 1.219 | 1.378 |
| 10 | 0.346 | 1.235 | 1.384 |
| 15 | 0.500 | 1.243 | 1.391 |
| 20 | 0.644 | 1.252 | 1.396 |
| 25 | 0.780 | 1.264 | 1.401 |

| CB/PA solutions | | | |
|-------------------------------|--------------------------------------|------------------------|-------|
| $w_{\text{CB}} / \text{wt}\%$ | $c_{\text{CB}} / \text{mol dm}^{-3}$ | $d / \text{g cm}^{-3}$ | n_2 |
| 0 | 0 | 1.271 | 1.399 |
| 5 | 0.178 | 1.276 | 1.426 |
| 10 | 0.343 | 1.295 | 1.438 |
| 15 | 0.496 | 1.299 | 1.432 |
| 20 | 0.641 | 1.314 | 1.431 |
| 25 | 0.773 | 1.320 | 1.422 |

| CL/PA solutions | | | |
|-------------------------------|---------------------------------------|------------------------|-------|
| $w_{\text{CL}} / \text{wt}\%$ | $c_{\text{CB}}' / \text{mol dm}^{-3}$ | $d / \text{g cm}^{-3}$ | n_2 |
| 2 | 0.075 | 1.240 | 1.423 |
| 4 | 0.147 | 1.245 | 1.431 |
| 6 | 0.219 | 1.253 | 1.433 |
| 8 | 0.289 | 1.269 | 1.435 |
| 10 | 0.362 | 1.287 | 1.437 |

Table S2. Compositions (number of CB, FA, and PA) of the systems for MD simulations, and density (d) in 20 wt% CB/FA and 20 wt% CB/PA solutions.

| Sample | CB(solvent) ₅ | FA | PA | $d / \text{g cm}^{-3}$ | |
|--------------|--------------------------|------|------|------------------------|-------------------|
| | | | | MD ^a | Exp. ^b |
| 20 wt% CB/FA | 139 | 4471 | - | 1.3583 | 1.261 |
| 20 wt% CB/PA | 139 | - | 2007 | 1.3397 | 1.314 |

^a Values obtained from the present MD simulations. ^b Experimental values.

Table S3. Coordination numbers $N(r)$ of O_H atoms of solvent molecules around O_X atoms of the CB(solvent)₅ molecules, obtained from MD simulations for 20 wt% CB/FA and CB/PA systems. The $N(r)$ was calculated by the integration of the corresponding $g_{\text{OX-OH}}(r)$ up to $r = 3.0 \text{ \AA}$, shown in Figure 11.

| O (solute)–O (solvent) | CB/FA system | CB/PA system |
|--------------------------------|--------------|--------------|
| O ₁ –O _H | 0.99 | 0.83 |
| O ₂ –O _H | 0.51 | 0.30 |
| O ₃ –O _H | 0.86 | 0.49 |
| O ₄ –O _H | - | 0.27 |
| Total | 2.36 | 1.89 |

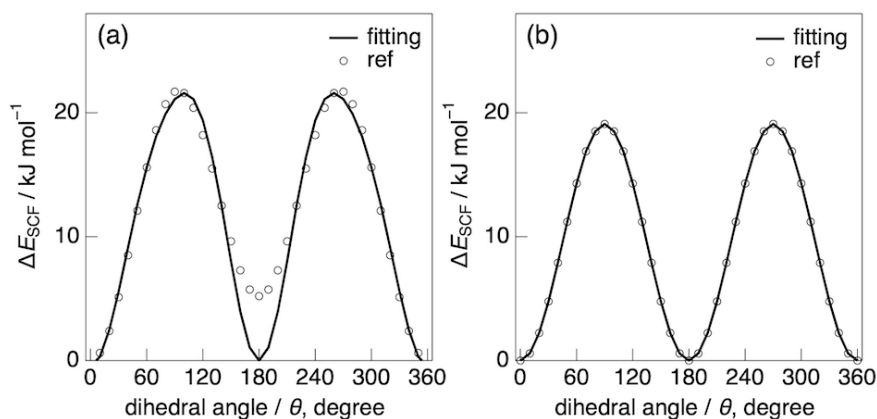


Figure S1. Torsion potential energy surface as a function of the (a) H–C–O–H and (b) O=C–O–H dihedral angle of FA molecule from ref 5 (open circles). The solid line shows the fitting result for the data using the following equation to determine the parameters V_n ($n = 1, 2, 3$, and 4). The resulting V_n values are: $V_1 = -0.5468$ kJ mol⁻¹, $V_2 = 5.2941$ kJ mol⁻¹, $V_3 = 0.6960$ kJ mol⁻¹, and $V_4 = 0.5412$ kJ mol⁻¹ for H–C–O–H; $V_1 = 0$ kJ mol⁻¹, $V_2 = 4.565$ kJ mol⁻¹, $V_3 = 0$ kJ mol⁻¹, and $V_4 = 0$ kJ mol⁻¹ for O=C–O–H.

$$E(\phi) = \frac{V_1}{2} [1 + \cos(\phi + f_1)] + \frac{V_2}{2} [1 - \cos(2\phi + f_2)] + \frac{V_3}{2} [1 + \cos(3\phi + f_3)] + \frac{V_4}{2} [1 - \cos(4\phi + f_4)] \quad (\text{S3}).$$

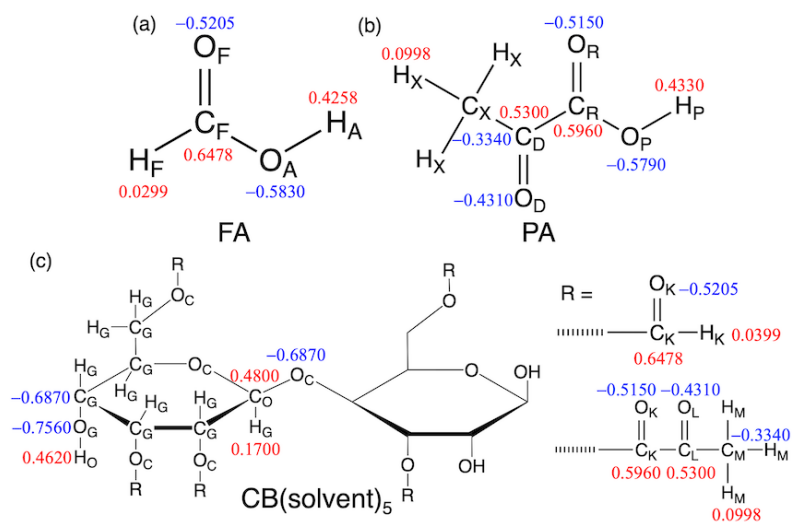


Figure S2. The partial charges of (a) FA, (b) PA and (c) CB(solvent)₅ were calculated based on the ChelpG method [MP2/cc-pVTZ(-f)/HF/6-31G(d)]. R is a substituent derived from an OH group, which is modified in the reactive solvent (FA or PA). In a formic acid system, the OH group is formylated, and the resulting R corresponds to a formyl group. In a pyruvic acid system, it is esterified, and R corresponds to an ester group.

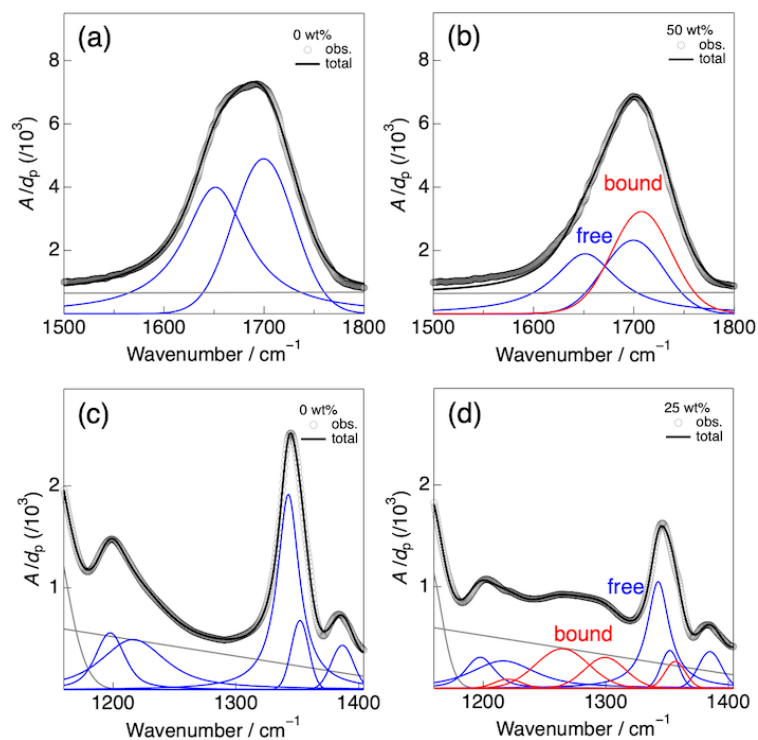


Figure S3. Full peak deconvolution into individual peaks for (a) neat FA and (b) 50 wt% CB/FA solution, (c) neat PA, and (d) 25 wt% CB/PA solution.

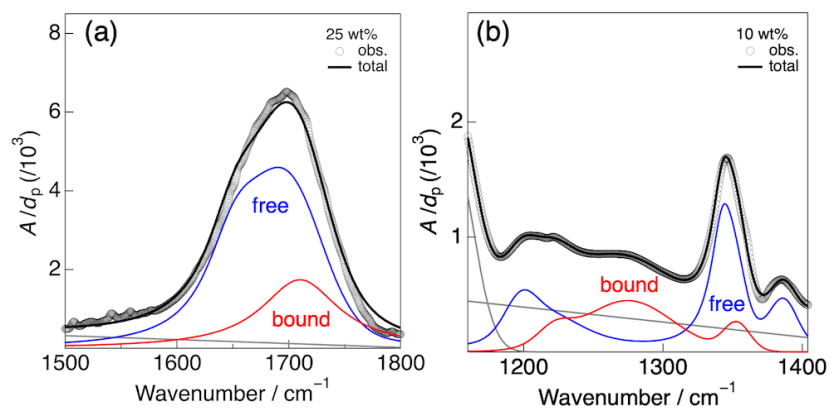


Figure S4. Typical peak deconvolution results for (a) 25 wt% CL/FA and (b) 10 wt% CL/PA solutions.

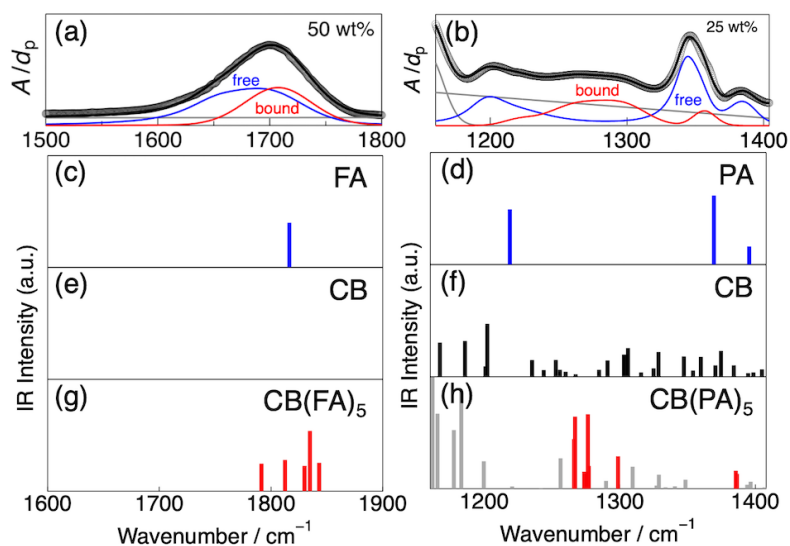


Figure S5. Typical peak deconvolution results for (a) 50 wt% CB/FA and (b) 25 wt% CB/PA solutions, and the theoretical IR bands for (c) FA, (d) PA, (e, f) CB, (g) CB(FA)_5 , and (h) CB(PA)_5 molecules.

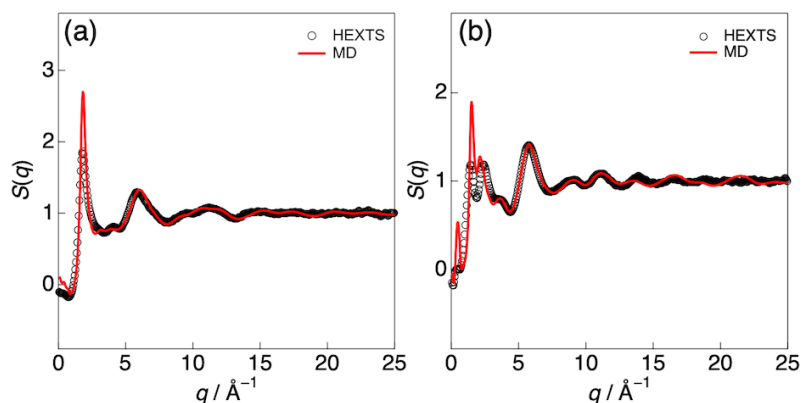


Figure S6. The X-ray structure factor $S(q)$ obtained from HEXTS experiments (open circles) and MD simulations (solid line) obtained for (a) 20 wt% CB/FA and (b) 20 wt% CB/PA solutions.

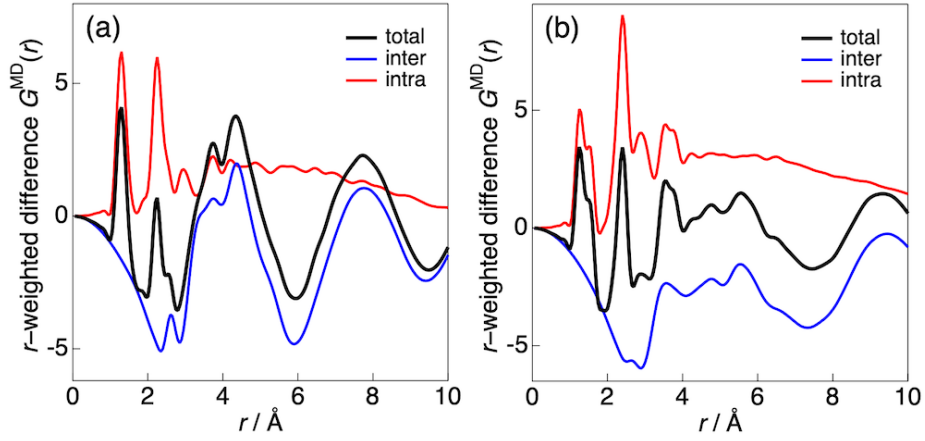


Figure S7. r^2 -weighted partial $G^{\text{MD}}(r)$ s for intramolecular [red; $G^{\text{MD}}_{\text{intra}}(r)$] and intermolecular [blue; $G^{\text{MD}}_{\text{inter}}(r)$] contributions, associated with the total profile [black; i.e., $G^{\text{MD}}_{\text{total}}(r) = G^{\text{MD}}_{\text{intra}}(r) + G^{\text{MD}}_{\text{inter}}(r)$], for (a) 20 wt% CB/FA and (b) 20 wt% CB/PA solutions.

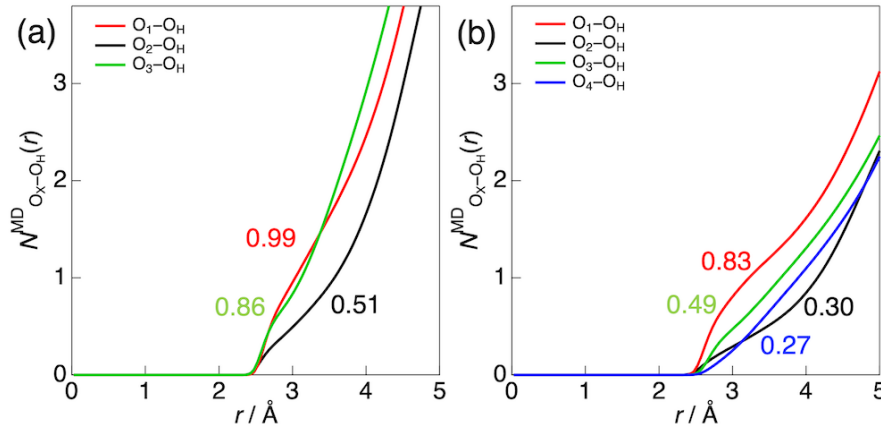


Figure S8. Coordination numbers $N(r)$ obtained by integrating the radial distribution functions $g_{\text{OX-OH}}(r)$ for $\text{CB}(\text{solvent})_5$ in (a) formic acid (FA) and (b) pyruvic acid (PA) systems. The curves represent the cumulative numbers of solvent O_H atoms around each oxygen site ($\text{O}_1\text{--O}_4$) in the chemically modified CB unit as a function of distance r . The coordination numbers at $r = 3.0$ Å, corresponding to the number of hydrogen bonds per oxygen site, are indicated in the figure and summarized in Table S3.

References

1. S. Sakai, *KEK Report 90-16*, National Laboratory for High Energy Physics, Tsukuba, Japan, 1990.

2. D. T. Cromer, *J. Chem. Phys.*, 1969, **50**, 4857-4859.
3. J. H. Hubbell, Wm. J. Veigele, E. A. Briggs, R. T. Brown, D. T. Cromer and R. J. Howerton, *J. Phys. Chem. Ref. Data*, 1975, **4**, 471-538.
4. K. Hirose, K. Fujii, K. Hashimoto and M. Shibayama, *Macromolecules*, 2017, **50**, 6509-6517.
5. N. Dawass, J. Langeveld, M. Ramdin, E. Perez-Gallent, A. A. Villanueva, E. J. M. Giling, J. Langerak, L. J. P. van den Broeke, T. J. H. Vlugt and O. A. Moultos, *J. Phys. Chem. B*, 2022, **126**, 3572-3584.